Journal of Engineering and Sustainable Development
www.jeasd.org
Vol. 20, No.05, September 2016
ISSN 2520-0917

A SUGGESTED ANALYTICAL SOLUTION TO DYNAMIC CHARACTERISTICS OF A PLATE DUE TO EFFECT THERMAL LOADING

Dr. Husam A. Kareem[1], Prof. Dr. Muhsin J. Jweeg[2], Prof. Dr. Shaker S. Hassan[3]

1) Department of Mechanical Engineering, University of Technology, Baghdad, Iraq.
2) Prostheses and Ortheses Engineering Department, College of Engineering, Al-Nahrain University, Baghdad, Iraq.
3) Department of Mechanical Engineering, University of Technology, Baghdad, Iraq.

Abstract: In order to find the effect of thermal loading on dynamic characteristics, a three dimensional steady state thermal analysis of thin rectangular plate subjected to heat flux extending over a specific region with convection boundary conditions was conducted. Analytical solution was suggested with the intention of assuring the result, which was used to study the variation of dynamic characteristics. The derivation of a closed form analytical solution of the heat equation for specific boundary condition and heat flux model was necessary to describe the three dimensional spatial temperature distributions which in turn were used to derive the required equation for the plate dynamics. Different plate dimensions were studied with heater location and shape was fixed, while its dimensions vary according to plate dimension under consideration. The numerical and experimental results were found to be comparable.

Keywords: *Dynamic; Heating load; Thermoplastic; Thin Plate*

الحل التحليلي المقترح لتأثير الأحمال الحرارية على الخواص الديناميكية للصفائح

الخلاصة: تم إيجاد الحل التحليلي بالأبعاد الثلاثة الواصف لتغير الخواص الديناميكية لصفيحة متعرضة لحمل حراري على جزء منها وتفقد الحرارة بواسطة الحمل الحراري . بهدف إيجاد وصف تحليلي لتأثير الحمل الحراري على أبعاد الصفيحة بصيغة مغلقة (Closed Form).تم دراسة صفائح بأبعاد مختلفة حيث تم تثبيت شكل المسخن وموقعه وتم تغيير عرضه وبما يتناسب وأبعاد الصفيحة . تم مقارنة النتائج التحليلية مع النتائج العددية و العملية ووجد أنها متقاربة.

1. Introduction

Danilovskay [1] investigated the dynamical thermoelasticity with a quick heating has been carried out. In his work, the strain deformation state of a half space with its surface heating has been observed. Manson [2] studied of a brief

*Corresponding Author husamalwan5@gmail.com

review of the classical continuum approach to thermoelasticity problems are given. It is shown that an analogous technique can be used to reduce the study of thermally induced vibrations by finite element techniques to that of a forced response analysis of the idealized structure excited by time dependent equivalent mechanical loads. Xiaogeng Tian [3] used the principle of virtual work, to derive the finite element equations corresponding to the generalized thermoelasticity with two relaxation times. In order to improve the accuracy of integral transform method, especially in two/three-dimension, the equations were solved directly in time-domain. As numerical examples, the developed method was used to investigate the generalized thermo elastic behavior of a slim strip and a semi-infinite plate subjected to thermal shock loading. Kulik [4] presented the temperature field during one source heating. If there is a system of heat energy sources, a solution to the transfer equations can't be obtained yet in the analytical form. In the sum of other works, the temperature fields and the stress strain states of plates and shells are characterized by a sudden increase of temperature and deflection. Also by a sudden jump of stresses in the place of the heat source. All of the mentioned components decrease rapidly in the neighborhood of the heat source. Due to the mathematical difficulties of finding an exact analytical solution to the three dimensional problems many researchers assume that the temperature changes linearly along a thickness.

Wael Rasheed [5] studied the theoretical approach on the theory of bending of isotropic thermo elastic thin plates to obtain the governing differential equation. By using the governing differential equation and the Rayleigh Ritz method of minimizing the total potential energy of a thermo elastic structural system, thermal buckling equations were established for rectangular plate with different fixing edge conditions and with different aspect ratio. The strain energy stored in a plate element due to bending, mid-plane thermal force and thermal bending was obtained. Expressions of the frequency equations for rectangular plate model with and without the thermo elastic effect for the cases (all edges are simply supported, all edges are clamped, and two opposite edges are clamped while others are simply supported) were obtained through direct method for simply supported ends and using Hamilton's principle with minimizing of Ritz method to total energy (strain and kinetic) for the rest of boundary conditions, also the plate thickness was taken as a design variable.

Al-Huniti [6] the resulting heat conduction equation was solved using semi analytically employing the Laplace transformation and the Riemann sum approximation to calculate the temperature distribution within the plate. The equation of motion of the plate was solved numerically using the finite difference technique to calculate the transient variations in deflections. Jeon [7] studied the experimental analysis on the free vibration characteristics of the rectangular aluminum plate under rapid thermal loading. The configuration of the plate was 100 x 100 x 2mm. Halogen lamps were used for the rapid thermal loading. The thermal loading was controlled by electric control system, and the test data was scanned by the laser scanning vibro-meter. The rate of thermal load on the plate was 2, 10, 30, 45, 60 and 70 °C/sec. The rectangular plate was hung using a bungee cord with a 7 mm dia. and steel cables were used to make a free-free boundary condition. One side of the rectangular plate was heated by Halogen lamps and electric

power. The experimental results showed that the fundamental natural frequency of the rectangular aluminum plate under rapid thermal loading (70 °C/sec) decreases about 8 % to that when under no thermal loading. In this work, the fundamental equations for the small- deflection of thermo-elastic bending of thin plates will be derived to obtain the thermal stresses that result from thermo-elastic effect and its effect on the natural frequencies and mode shapes. The analytical solution is divided into two parts. First part is concerned with thermal problem while the second part is focused on dynamic characteristics. The results compared with experimental published in Ph.D. thesis [8].

2-Solution of Thermal Problem

When the boundaries of a multi-dimensional conduction problem correspond to the coordinate surfaces in a system of orthogonal coordinates, such as Cartesian, an exact solution by analytical methods becomes possible. One common method is based on the separation of variables, another on the Laplace transforms or the operational calculus.

Consider the steady-state three dimensional homogenous conduction with no heat generation rectangular coordinate system [9].

$$\frac{\partial^2\theta}{\partial x^2}+\frac{\partial^2\theta}{\partial y^2}+\frac{\partial^2\theta}{\partial z^2}=0 \tag{1}$$

Let θ^{∞} temperature increasing and

$$\theta^{\infty}{}_{(x,y,z)}=T_{(x,y,z)}-T_{\infty} \tag{2}$$

Where T_{∞} Temperature constant, then

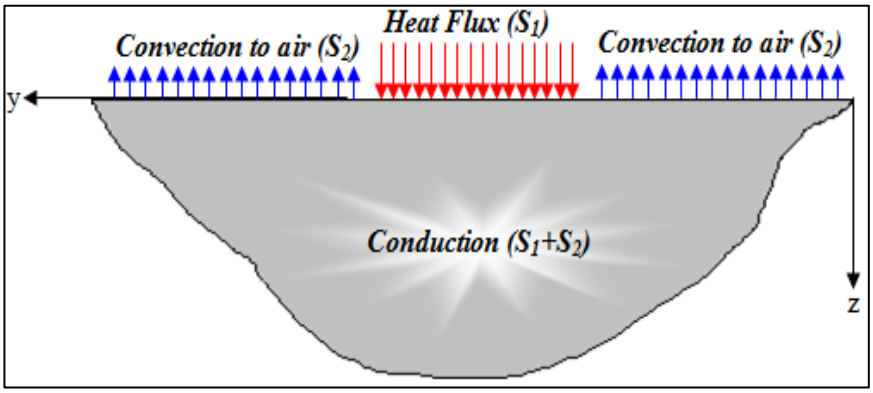

Fig.1: Thermal boundary condition zones of upper plate surface showing conduction, convection, and heat flux zones

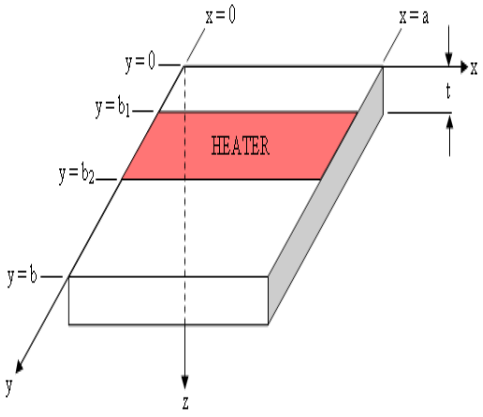

Fig.2: Heater location on the upper

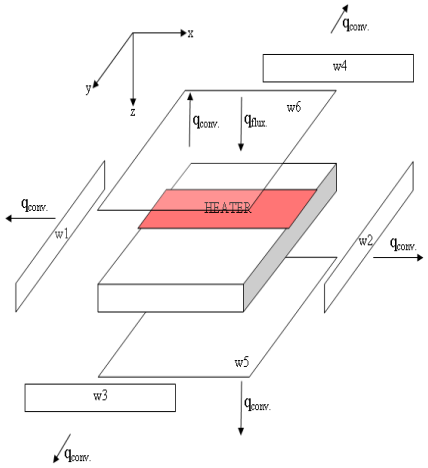

Fig.3: Description of thermal

Applied boundary condition for wall 6 (upper surface) at Z=0

Energy method concepts were used to derive the governing equation of this boundary condition. Hence, for the upper surface the energy balance requires that showing in Fig. 1, and Table1. Figs.1 And 3 show the heater location and thermal boundary conditions.

Table1:Zones of convection and heat flux boundary conditions

Wall	zone	x-range	y-range	z-range	Thermal Boundary Condition
W6	S2	0≤x≤a	$0 \le y \le b_1$	z=0	Convection only
	S1		$b_1 \le y \le b_2$		Heat Flux
	S2		$b_2 \le y \le b$		Convection only

$$\left\{\begin{matrix} Conducted \\ Heat \end{matrix}\right\}_{S1+S2} = \left\{\begin{matrix} Heat & Flux \\ Gained & from \\ Heater & \end{matrix}\right\}_{S1} - \left\{\begin{matrix} Heat & Loss \\ by & Convection \\ to & Air \end{matrix}\right\}_{S2} \quad (3)$$

$$-K\left.\frac{\partial T}{\partial z}\right|_{S1+S2} = q(x,y)\big|_{S1} - h(T_{w6} - T_{\infty})\big|_{S2}$$

$$-K\left.\frac{\partial \theta}{\partial z}\right|_{S1+S2} + h\theta\big|_{S2} = q(x,y)_{S1} \qquad (4)$$

Equation (1) could be solved by separation of variables [6].

Since

$$\theta(x,y,z) = \sum_{n=0}^{\infty} \sum_{m=0}^{\infty} \bar{\theta}_{n,m} \quad \overline{\varphi_n}(x) \quad \overline{\psi_m}(y) \quad \overline{\Gamma_{n,m}}(z) \qquad (5)$$

Where

$$\overline{\varphi}(x) = \sin(\alpha x + \varepsilon_{\alpha}), \overline{\psi}(y) = \sin(\beta y + \varepsilon_{\beta}), \overline{\Gamma_{n,m}}(z) = e^{-\lambda_{n,m} z} + \frac{\lambda_{n,m} - h/k}{\lambda_{n,m} + h/k} e^{\lambda_{n,m}(z-2t)}$$

Where

$$\varepsilon_{\alpha} = \tan^{-1}\left(\frac{k}{h}\alpha_n\right) \qquad \text{and} \qquad \varepsilon_{\beta} = \tan^{-1}\left(\frac{k}{h}\beta_m\right)$$

$$\bar{\theta}_{n,m} = \frac{q_o \bar{I}1}{h\overline{\Gamma_{n,m}}(z=0)\bar{I}2 - K\left.\frac{\partial \overline{\Gamma_{n,m}}(z)}{\partial z}\right|_{z=0} \bar{I}3} \qquad (6)$$

$$\therefore \quad \theta_{(x,y,z)} = \sum_{n=0}^{\infty}\sum_{m=0}^{\infty} \theta_{nm}\left(\sin(\alpha_n x) + \frac{K}{h}\alpha_n \cos(\alpha_n x)\right)$$

$$(\sin(\beta_m y) + \frac{k}{h}\beta_m \cos(\beta_m y).[e^{-\lambda z} + \frac{\left(\lambda - \frac{h}{k}\right)}{\left(\lambda + \frac{h}{k}\right)} e^{\lambda(Z-2t)}] \qquad (7)$$

Which is applicable for $0 \le x \le a$, $0 \le y \le b$, *and* $0 \le z \le t$

3- Strain Energy of Plates

The energy method can be very advantageous, to deriving expression, assuming that the in-plane stress resultants are entirely due to external edge loading in the plane of the plate, in which case they are unchanged during bending. Strain energy of the plate middle surface can be obtained from the general expression of the potential energy of an elastic body it is simplified and has the following form for the above mentioned increment of the middle surface. The Lagrangian (L) of the plate can be written as: (7)

$$L = \frac{1}{2}\iint_A D\left(\frac{\partial^2 w}{\partial x^2}+\frac{\partial^2 w}{\partial y^2}\right)^2 dxdy - \frac{1}{2}\iint_A \left\{ N_x\left(\frac{\partial w}{\partial x}\right)^2 + N_y\left(\frac{\partial w}{\partial y}\right)^2 + 2N_{xy}\left(\frac{\partial w}{\partial x}\right)\left(\frac{\partial w}{\partial y}\right) \right\} dxdy$$
$$+ \iint_A \frac{M_t}{1-\nu}\left(\frac{\partial^2 w}{\partial x^2}+\frac{\partial^2 w}{\partial y^2}\right) dxdy - \frac{1}{2}\iint_R \rho h \dot{w}^2 dxdy \quad (8)$$

The free vibration solution may be assumed as:

$$w(x,y,t) = \sum_{i=1}^{m}\sum_{j=1}^{n} A_{ij} X_i(x) Y_j(y) \sin \omega t \quad (9)$$

Substituting (9) into Lagrangian (8) and minimizing the resulting with respect to A_{ij} , gives

$$\sum_{k=1}^{m}\sum_{j=1}^{n}\left[\begin{array}{l} D\int_0^a\int_0^b \left((X'')^2Y^2 + 2X''XY''Y + X^2(Y'')^2\right)dxdy \\ -\int_0^a\int_0^b \left(N_x(X')^2Y^2 + N_y X^2(Y')^2 + 2N_{xy}XX'YY'\right)\,dxdy \end{array}\right] A_{ij} + \sum_{i=1}^{m}\sum_{j=1}^{n}\frac{M_t}{(1-\nu)}\int_0^a\int_0^b (X''Y + XY'')dxdy$$
$$= \sum\sum\left[\rho t\omega^2\int_0^a\int_0^b X^2Y^2 dxdy\right]A_{ij} \quad (10)$$

Comparing (10) with the Eigen value problem $\left[K-\omega^2 M\right]\{A\} = \{F\} \rightarrow$

$$\left|K-\omega^2 M\right| = 0$$

$$\omega_{ij}^2 = \frac{D\int_0^a\int_0^b \left((X_i'')^2Y_j^2 + 2X_i''X_iY_j''Y_j + X_i^2(Y_j'')^2\right)dxdy \;-\; \int_0^a\int_0^b \left(N_x(X_i')^2Y_j^2 + N_y X_i^2(Y_j')^2 + 2N_{xy}X_iX_i'Y_jY_j'\right)\,dxdy}{\rho t\int_0^a\int_0^b X_i^2Y_j^2 dxdy} \quad (11)$$

Equation (11) is the general frequency equation**.**

$$\because N_{xy} = \frac{E}{2(1+\nu)}\left(\frac{\partial u}{\partial y}+\frac{\partial v}{\partial x}\right) = 0 \text{ (At all fixing edge boundary conditions)}$$

Simplification (11) gives:

$$\omega_{ij}^2 = \frac{D\left(\int_0^a (X_i'')^2 dx\int_0^b Y_j^2 dy + 2\int_0^a X_i''X_i dx\int_0^b Y_j''Y_j dy + \int_0^a X_i^2 dx\int_0^b (Y_j'')^2 dy\right) \;-\; \int_0^a\int_0^b N_x(X_i')^2Y_j^2 dxdy - \int_0^a\int_0^b N_y X_i^2(Y_j')^2 dxdy}{\rho t\int_0^a X_i^2 dx\int_0^b Y_j^2 dy} \quad (12)$$

For Stress free vibration (i.e. Nx=Ny=0)

$$\omega_{ij}^2\Big|_{free} = \frac{D\left(\int_0^a (X_i^{"})^2 dx \int_0^b Y_j^2 dy + 2\int_0^a X_i^{"} X_i dx \int_0^b Y_j^{"} Y_j dy + \int_0^a X_i^2 dx \int_0^b (Y_j^{"})^2 dy\right)}{\rho t \int_0^a X_i^2 dx \int_0^b Y_j^2 dy} \tag{13}$$

$$\omega_{ij}^2 = \omega_{ij}^2\Big|_{free} + \frac{\int_0^a \int_0^b N_x (X_i^{'})^2 Y_j^2 dxdy + \int_0^a \int_0^b N_y X_i^2 (Y_j^{'})^2 dxdy}{\rho t \int_0^a X_i^2 dx \int_0^b Y_j^2 dy} \tag{14}$$

The last term could be designated as:

$$\omega_{ij}^2\Big|_{Stress} = \frac{\int_0^a \int_0^b N_x (X_i^{'})^2 Y_j^2 dxdy + \int_0^a \int_0^b N_y X_i^2 (Y_j^{'})^2 dxdy}{\rho t \int_0^a X_i^2 dx \int_0^b Y_j^2 dy} \tag{15}$$

Hence $$\omega_{ij}^2 = \omega_{ij}^2\Big|_{free} + \omega_{ij}^2\Big|_{Stress}$$

4- Incorporating Temperature Distribution

Recall that

$$\because \theta(x,y,z) = T(x,y,z) - T_\infty = \sum_{n=0}^{\infty} \sum_{m=0}^{\infty} \bar{\theta} n,m \quad \overline{\varphi_n}(x) \quad \overline{\psi_m}(y) \quad \overline{\Gamma_{n,m}}(z)$$

Where $\theta_{n,m} = T(x,y,z) - T_\infty$,

$$T(x,y,z) = T_\infty + \theta(x,y,z) \tag{16}$$

$$\therefore T(x,y,z) = T_\infty + \sum_{n=0}^{\infty} \sum_{m=0}^{\infty} \bar{\theta} n,m \quad \overline{\varphi_n}(x) \quad \overline{\psi_m}(y) \quad \overline{\Gamma_{n,m}}(z) \tag{17}$$

Since $\Delta T = T(x,y,z) - T_o$

Assuming that $T_o = T_\infty$ (initial plate temperature equals to ambient temperature which is constant)

$$\Rightarrow \begin{matrix} \Delta T = T(x,y,z) - T_\infty \\ \Delta T \quad = \theta(x,y,z) \end{matrix}$$

$$\therefore \Delta T = \sum_{n=0}^{\infty} \sum_{m=0}^{\infty} \bar{\theta} n,m \quad \overline{\varphi_n}(x) \quad \overline{\psi_m}(y) \quad \overline{\Gamma_{n,m}}(z) \tag{18}$$

$$\because N_x = N_y = -\frac{N_t}{1-\upsilon} \text{ Where } N_t = \alpha E \int_0^t (\Delta T) dz$$

$$N_x = N_y = -\frac{\alpha E}{1-\upsilon} \left(\sum_{n=0}^{\infty} \sum_{m=0}^{\infty} \bar{\theta} n,m \quad \overline{\varphi_n}(x) \quad \overline{\psi_m}(y) \quad \overline{\Gamma_{n,m}}(t)\right) \tag{19}$$

Where: $$\overline{\Gamma_{n,m}}(t)=\int_0^t \overline{\Gamma_{n,m}}(z)dz$$

$$=\frac{-1}{\lambda_{n,m}}(e^{-\lambda_{n,m}t}-1)+\frac{1}{\lambda_{n,m}}\frac{\lambda_{n,m}-h/k}{\lambda_{n,m}+h/k}(e^{-\lambda_{n,m}t}-e^{-2\lambda_{n,m}t})$$

Can rewriting (13) in form

$$\omega_{ij}^2\big|_{free}=\frac{D(I_1I_2+2I_3I_4+I_5I_6)}{\rho tI_7I_8} \tag{20}$$

Where I's are given in Table2.

$$\text{In}\ \omega_{ij}^2\big|_{Stress}=\frac{\int_0^a\int_0^b N_x(X_i')^2Y_j^2dxdy+\int_0^a\int_0^b N_yX_i^2(Y_j')^2dxdy}{\rho t\int_0^a X_i^2dx\int_0^b Y_j^2dy}$$

$$\int_0^a\int_0^b N_x(X_i')^2Y_j^2dxdy=\int_0^a\int_0^b-\frac{\alpha E}{1-\upsilon}(\sum_{n=0}^{\infty}\ \sum_{m=0}^{\infty}\bar{\theta}_{n,m}\ \ \overline{\varphi_n}(x)\ \ \overline{\psi_m}(y)\ \ \overline{\Gamma_{n,m}}(t))(X_i')^2Y_j^2dxdy$$

$$=-\frac{\alpha E}{1-\upsilon}(\sum_{n=0}^{\infty}\ \sum_{m=0}^{\infty}\bar{\theta}_{n,m}\ \ \int_0^a\overline{\varphi_n}(x)(X_i')^2dx\ \ \int_0^b\overline{\psi_m}(y)Y_j^2dy\ \ \overline{\Gamma_{n,m}}(t)) \tag{21}$$

Where $$\int(\sum f(x))dx=\sum(\int f(x)dx)$$

$$\int_0^a\int_0^b N_yX_i^2(Y_j')^2dxdy=\int_0^a\int_0^b-\frac{\alpha E}{1-\upsilon}(\sum_{n=0}^{\infty}\ \sum_{m=0}^{\infty}\bar{\theta}_{n,m}\ \ \overline{\varphi_n}(x)\ \ \overline{\psi_m}(y)\ \ \overline{\Gamma_{n,m}}(t))X_i^2(Y_j')^2dxdy$$

$$=-\frac{\alpha E}{1-\upsilon}(\sum_{n=0}^{\infty}\ \sum_{m=0}^{\infty}\bar{\theta}_{n,m}\ \ \int_0^a\overline{\varphi_n}(x)X_i^2dx\ \ \int_0^b\overline{\psi_m}(y)(Y_j')^2dy\ \ \overline{\Gamma_{n,m}}(t)) \tag{22}$$

By substituting (21) and (22) into (15) obtain:

$$\therefore\ \omega_{ij}^2\big|_{Stress}=-\frac{\alpha E}{1-\upsilon}\frac{\sum_{n=0}^{\infty}\ \sum_{m=0}^{\infty}\bar{\theta}_{n,m}\ \ \{I9\ \ I10\ +\ I11\ \ I12\}\ \ \overline{\Gamma_{n,m}}(t)}{\rho tI_7I_8} \tag{23}$$

Where I's are given in Table2

Table 2:Definition of I_s integration solutions

$I_1=\int_0^a(X_i'')^2dx$	$I_4=\int_0^b Y_j''Y_jdy$	$I_7=\int_0^a X_i^2dx$	$I10=\int_0^b\overline{\psi_m}(y)Y_j^2dy$
$I_2=\int_0^b Y_j^2dy$	$I_5=\int_0^a X_i^2dx$	$I_8=\int_0^b Y_j^2dy$	$I11=\int_0^a\overline{\varphi_n}(x)X_i^2dx$
$I_3=\int_0^a X_i''X_idx$	$I_6=\int_0^b(Y_j'')^2dy$	$I9=\int_0^a\overline{\varphi_n}(x)(X_i')^2dx$	$I12=\int_0^b\overline{\psi_m}(y)(Y_j')^2dy$

5- Shape Functions were used [10]

Four fully clamped (CCCC) edges (i.e. at x=0 and x=a)
Even Modes are given by

$$X(x) = \cos(\gamma_i(\frac{x}{a} - \frac{1}{2})) + \frac{\sin(\frac{\gamma_i}{2})}{\sinh(\frac{\gamma_i}{2})}\cosh(\gamma_i(\frac{x}{a} - \frac{1}{2}))$$

$$where \quad m = 2,4,6... \tag{24}$$

$$and \quad \tan(\frac{\gamma_i}{2}) + \tanh(\frac{\gamma_i}{2}) = 0$$

While odd Modes are given by

$$X(x) = \sin(\gamma_i(\frac{x}{a} - \frac{1}{2})) + \frac{\sin(\frac{\gamma_i}{2})}{\sinh(\frac{\gamma_i}{2})}\sinh(\gamma_i(\frac{x}{a} - \frac{1}{2}))$$

$$where \quad m = 1,3,5... \tag{25}$$

$$and \quad \tan(\frac{\gamma_i}{2}) - \tanh(\frac{\gamma_i}{2}) = 0$$

The function $Y_{(y)}$ are similarly chosen by the conditions at y=0 and y=b by replacing X by Y, a by b, and m by n in (24) and (25).

5.1. Four edges fully clamped (CCCC) (stress free)

To calculate the natural frequency without heating load (stress free) for boundary condition (four edge fully clamped) CCCC, (13) was used for stress free. Mode shape functions (24) and (25) were substituted in (13).The integration solutions as shown in Table 2 were substituted in (20) and then solved by MATLAB program to obtain final results of natural frequency (stress free).

5.2. Four edges fully clamped (CCCC) (under thermal stress)

To calculate the natural frequency due to heating load effect for boundary conditions (four edge fully clamped) CCCC, (15) was used to find natural frequency under thermal stress, (19) was used for thermal force (N_t).Mode shape functions (24)and (25) were substituted in (15).The integration solutions as shown in Table 2 were substituted in (23) and then solved by MATLAB program to obtain final results of natural frequencies (thermally stress).

6-Results and discussions

The three dimensional steady-state heat transfer problem of a rectangular plate made from aluminum alloy 7075 T6, was analyzed by using three methods which are

analytical, numerical, and experimental [8]. The results then compared and found comparable. Solution of (1) analytically takes another form when it is applied to the thermal boundary conditions and will gives the temperature in a three-dimensional body as a function of the three independent space coordinates x, y and z.

Thermal Distribution for Plate dimensions (150*300* 2) mm , (200*300*2) mm, (250*300*2) mm and (300*300*2) mm and boundary conditions (CCCC) as shown in Table 3, Table 4 , Table 5 ,and Table 6 listed the variation of temperature distribution produced by the effect of applying different values of heating load up to Vanishing Heating Load (VHL) along y-axis at x=a/2 (CCCC).In order to reach VHL that which causes vanish natural frequency till to reach zero value, the following conclusions can be obtained for the same aspect ratio:

1-Smaller plates need more heat flux (q).
2- An increase in aspect ratio (b/a) at constant (b) led to heat flux (q) increasing.
3-CCCC needs less heat flux (q) than CSCS [8].
4-CSCS needs less heat flux (q) than CSSS [8].
5-CSSS needs less heat flux (q) than SSSS [8].

That mean as more restricting boundary condition is used then less values of heating load will be needed to reach VHL. This is because CCCC is restricted in plane displacements hence increasing in plane stresses. Tables 7 to Table 10 show the relationship between heating load and it is effect on natural frequency for boundary condition (CCCC) and for different plate dimensions (Analytically).The results were obtained by solving the analytical solutions by MATLAB. Fig.4 to Fig.7 show the effect of heating load on dynamic characteristic for different plate dimensions.

Fig.8 to Fig.11 show the charts of heating load effect on the natural frequencies and how to vanish mode shape one after the other for the first five natural frequencies ,with plate dimensions (150*300*2) mm, (200*300*2) mm ,(250*300*2) mm , (300*300*2) mm ,and boundary condition (CCCC).It was concluded from the obvious results the drift in mode number and vanishing natural frequency by the effect of increasing heating load, and any increasing in heating load (at the same boundary condition) will make a decreasing in the natural frequency, physically, applying heating load on plate will cause a decrease in stiffness of the plate's material, dynamically when stiffness of material decreases the natural frequency was decreased to.

As more restricting (clamped) boundary conditions is used, natural frequency will increase. Vic versa, as more unrestricting (simple support) boundary conditions is used, natural frequency will decrease. At the same time it can be seen that any increasing in plate dimensions will decreases the natural frequency, that means natural frequency is increased with aspect ratio increasing, this is because of a smaller plate which needs less heating load and still it has a higher stiffness.

Table 3: Variation of temperature distribution along y-axis at x=a/2 for plate dimension (150*300*2) mm and boundary condition CCCC (Numerical, Analytical and Experimental)

Heat Flux W/m^2		*T.C1 (C^o) 125mm*	*T.C2(C^o) 160mm*	*T.C3(C^o) 195mm*	*T.C4(C^o) 230mm*	*T.C5 (C^o) 265mm*
1800	Num.	46.522	36.545	37.522	39.241	42.195
	Ana.	46.71954	37.98706	38.76772	39.91218	42.31287
	Exp.	45	36	37	38	40.5
1900	Num.	47.329	36.798	37.828	39.644	42.761
	Ana.	47.53729	38.31967	39.1437	40.35175	42.88581
	Exp.	46	37	38.3	39.5	43
2700	Num.	53.783	38.818	40.282	42.862	47.292
	Ana.	54.07931	40.98059	42.15158	43.86827	47.46931
	Exp.	52.9	38.4	40.9	42	46.8
3500	Num.	60.237	40.838	42.737	46.08	51.823
	Ana.	60.62132	43.6415	45.15945	47.3848	52.05281
	Exp.	58	40	42	46	51
3700	Num.	61.851	41.343	43.35	46.885	52.956
	Ana.	62.25683	44.30673	45.91142	48.26393	53.19868
	Exp.	60.2	40.2	42	45.8	51

Table 4: Variation of temperature distribution along y-axis at x=a/2 for plate dimension (200*300*2) mm and boundary condition CCCC (Numerical, Analytical and experimental)

Heat Flux W/m^2		*T.C1 (C^o) 125mm*	*T.C2(C^o) 160mm*	*T.C3(C^o) 195mm*	*T.C4(C^o) 230mm*	*T.C5 (C^o) 265mm*
1200	Num.	35.105	35.779	36.969	39.02	42.027
	Ana.	35.99445	36.5162	37.28185	38.88515	41.82449
	Exp.	33.9	34.9	35	37	40
1300	Num.	35.364	36.094	37.383	39.605	42.863
	Ana.	36.32732	36.89255	37.722	39.45892	42.6432
	Exp.	34.4	35.6	36	38	40.9
1900	Num.	36.917	37.984	39.868	43.115	47.876
	Ana.	38.32454	39.15065	40.36293	42.90149	47.55545
	Exp.	35	35.6	36.7	41	45.7
2200	Num.	37.693	38.929	41.11	44.87	50.383
	Ana.	39.32315	40.2797	41.68339	44.62278	50.01157
	Exp.	36.9	38	40	43.7	48.8
2700	Num.	38.987	40.503	43.181	47.795	54.561

	Ana.	40.9875	42.16145	43.88416	47.4916	54.10511
	Exp.	37.9	39	42	45.8	53

Table 5: Variation of temperature distribution along y-axis at x=a/2 for plate dimension (250*300*2) mm and boundary condition CCCC (Numerical, Analytical and experimental)

Heat Flux W/m^2		*T.C1 (C^o) 125mm*	*T.C2(C^o) 160mm*	*T.C3(C^o) 195mm*	*T.C4(C^o) 230mm*	*T.C5 (C^o) 265mm*
800	Num	34.101	34.561	35.374	36.776	38.829
	Ana.	34.66121	35.00921	35.52016	36.58895	38.54688
	Exp.	33.7	34.2	35	36	38
900	Num	34.363	34.881	35.795	37.373	39.683
	Ana.	34.99386	35.38536	35.96018	37.16257	39.36524
	Exp.	34	34.7	35.4	37	38.8
1500	Num	35.939	36.801	38.326	40.955	44.805
	Ana.	36.98977	37.64227	38.60029	40.60429	44.27539
	Exp.	35	35.9	38	39.7	43.5
1600	Num	36.201	37.121	38.747	41.552	45.658
	Ana.	37.32242	38.01842	39.04031	41.17791	45.09375
	Exp.	36	36.4	38.5	40.4	44.2
2350	Num	38.17	39.522	41.91	46.03	52.061
	Ana.	39.81731	40.83956	42.34046	45.48005	51.23145
	Exp.	37.7	39	40. 9	45	50.6

Table 6: Variation of temperature distribution along y-axis at x=a/2 for plate dimension (300*300*2)mm and boundary condition CCCC(Numerical , Analytical and Experimental)

Heat Flux W/m^2		*T.C1 (C^o) 125mm*	*T.C2(C^o) 160mm*	*T.C3(C^o) 195mm*	*T.C4(C^o) 230mm*	*T.C5 (C^o) 265mm*
700	Num.	33.857	34.267	34.991	36.239	38.062
	Ana.	34.32532	34.62962	35.07655	36.01078	37.72135
	Exp.	33	33.5	34	35	36.7
750	Num.	33.99	34.429	35.204	36.542	38.495
	Ana.	34.49141	34.81745	35.29631	36.29727	38.13002
	Exp.	33.3	33.8	34.3	35.3	37
1200	Num.	35.184	35.886	37.127	39.267	42.391
	Ana.	35.98626	36.50793	37.27409	38.87563	41.80803
	Exp.	34.5	35	36	38	41
1300	Num.	35.449	36.209	37.554	39.872	43.257
	Ana.	36.31845	36.88359	37.7136	39.4486	42.62536

	Exp.	35	35.5	36.5	38.7	41.8
1875	Num.	36.974	38.071	40.011	43.354	48.237
	Ana.	38.22853	39.04363	40.24077	42.74317	47.32504
	Exp.	36	37	39	42	47

Table 7: CCCC, a=150 mm Effect of heating load on natural frequency (Hz) analytically

Mode No. i	j	0 W/m^2	1037.001 W/m^2	2074.003 W/m^2	2440.685 W/m^2	3042.213 W/m^2	4322.892 W/m^2	5089.862 W/m^2
1	1	538.6451	380.8796	0	0	0	0	0
1	2	698.4748	529.6994	270.7322	0	0	0	0
1	3	982.8129	797.9142	554.4481	437.0227	0	0	0
2	1	1402.388	1222.665	1011.498	925.3682	763.3101	0	0
2	2	1560.889	1392.835	1201.502	1126.093	990.0259	605.9099	0

Table 8: CCCC, a=200 mm Effect of heating load on natural frequency (Hz) analytically

Mode No i	j	0 W/m^2	617.9274 W/m^2	1235.855 W/m^2	1704.841 W/m^2	2473.023 W/m^2	2494.011 W/m^2	3116.307 W/m^2
1	1	333.0307	235.4882	0	0	0	0	0
1	2	515.0379	411.2395	270.1328	0	0	0	0
1	3	821.8194	711.7795	581.2684	458.0305	0	0	0
2	1	815.9529	707.6882	579.5396	458.9878	74.8509	0	0
2	2	986.462	883.2618	766.2869	663.889	448.1894	440.8175	0

Table 9: CCCC, a=250 mm Effect of heating load on natural frequency (Hz) analytically

Mode No i	j	0 W/m^2	443.2568 W/m^2	886.5135 W/m^2	1431.127 W/m^2	1663.957 W/m^2	2261.068 W/m^2	2265.711 W/m^2
1	1	242.7624	171.659	0	0	0	0	0
1	2	439.5593	365.198	271.1582	0	0	0	0
2	1	546.8608	468.3929	373.8008	204.5621	0	0	0
2	2	728.8611	653.5253	568.2886	441.5822	374.5549	0	0
1	3	756.236	678.24	590.0222	458.9761	389.7306	34.23314	0

Table 10: CCCC, a=300 mm Effect of heating load on natural frequency (Hz) analytically

Mode No i	j	0 W/m^2	361.525 W/m^2	723.05 W/m^2	1226.812 W/m^2	1311.2 W/m^2	1834.143 W/m^2	2054.248 W/m^2
1	1	197.2749	139.4944	0	0	0	0	0
2	1	402.8532	338.328	258.1491	0	0	0	0
1	2	402.8532	342.8466	269.809	102.2001	0	0	0
2	2	594.6867	532.8644	462.857	342.2033	317.5403	0	0
3	1	723.8035	657.033	582.6604	459.3685	435.314	236.9238	0

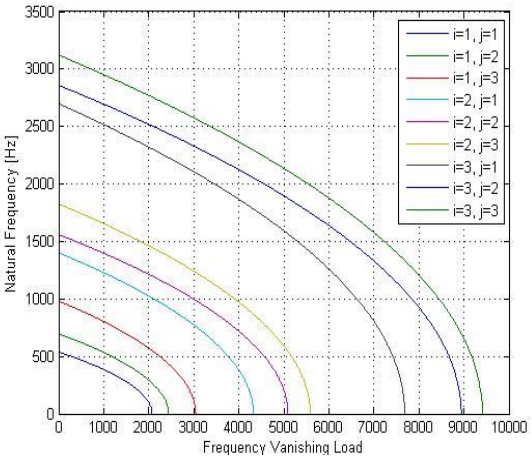

Fig.4:Effect of heating load (w/m^2) on natural frequency (Hz), Analytically, cccc, a=150

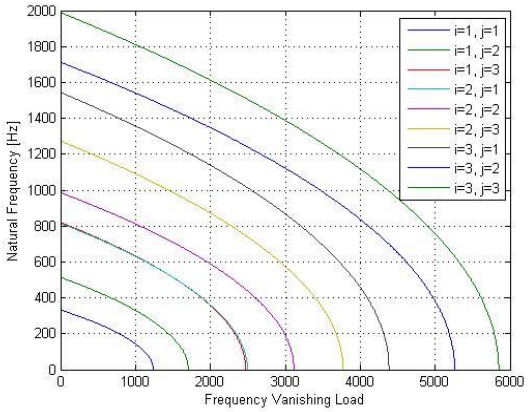

Fig (5): Effect of heating load (w/m^2) on natural frequency (Hz), Analytically, cccc, a=200

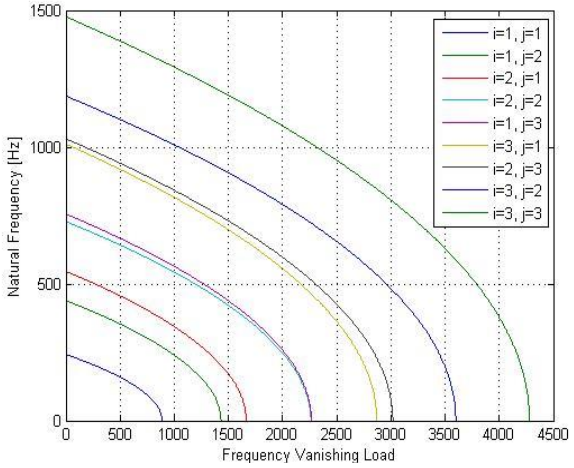

Fig.6: Effect of heating load (w/m^2) on natural frequency (Hz), Analytically, cccc, a=250

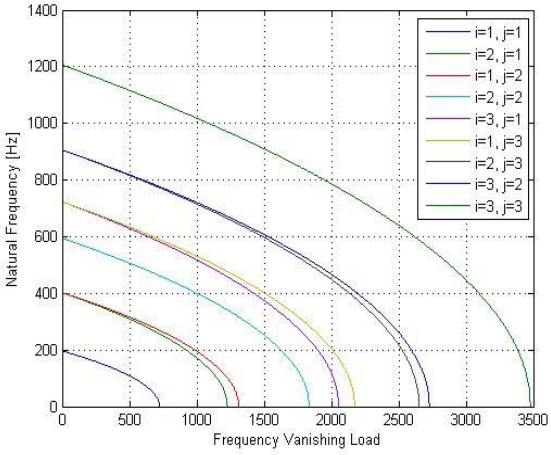

Fig.7: Effect of heating load (w/m^2) on natural frequency (Hz), Analytically, cccc, a=300

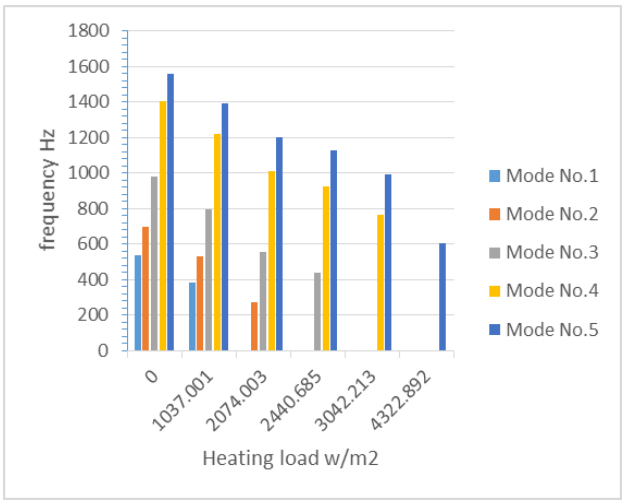

Fig (8): Effect of heating load on natural frequency up to vanishing heating load, CCCC, a=150 mm

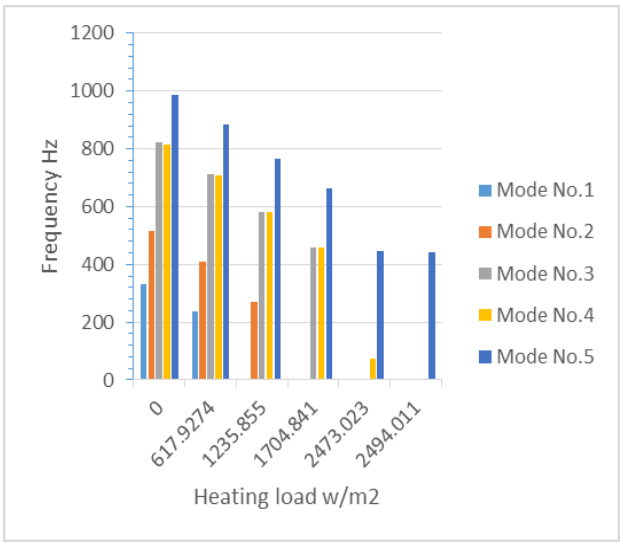

Fig (9): Effect of heating load on natural frequency up to vanishing heating load, CCCC, a=200 mm

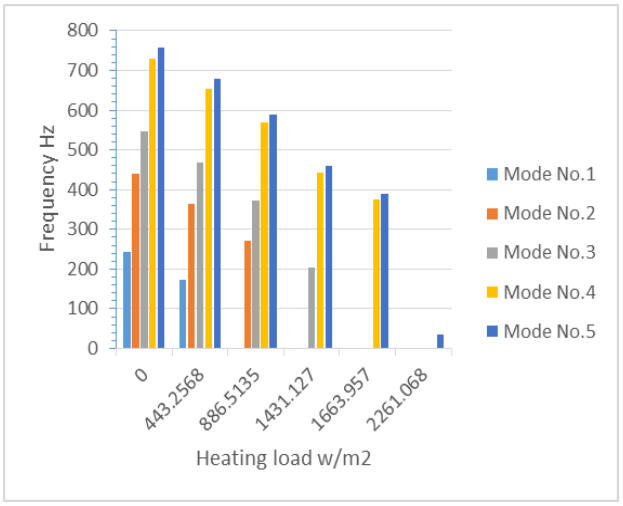

Fig (10): Effect of heating load on natural frequency up to vanishing heating load, CCCC, a=250 mm

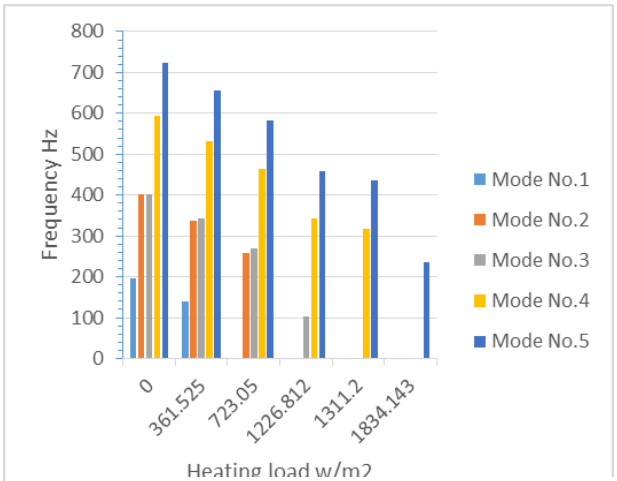

Fig (11): Effect of heating load on natural frequency up to vanishing heating load, CCCC, a=300 mm

Symbol list

Symbol	Meaning	Units
A	Area	m^2
a , b	Plate side length	m
D	Flexural rigidity of an isotropic plate	N.m
E	Modulus of elasticity of an isotropic material	N/m^2
h	Convection heat transfer coefficient	W/m ^oC
i,j	Integer	
K	Thermal conductivity	W/m ^oC
M_t	Thermal bending moment	N.m
M_x, M_y	Bending moment in x, y direction	N.m
ρ	Density of material	$N.m^2$
m,n	Integers representing the number of half-waves of the mode shapes in the x and y directions.	
N_x, N_y	Edge forces per unit length	N/m
N_{xy}	Shearing forces per unit length	N/m
N_t	Thermal forces per unit length	N/m
q	Heat flux	W/m
W	Shape function	
X_i , Y_j	Shape functions in x,y directions	
$\theta_{n,m}$	Difference of temperature distribution = ΔT	^oC
υ	Poisson ratio	
α_m, β_n	Root Coefficients	
ω_{ij}^2	Final natural frequency	Hz

6. Conclusions

1. A Smaller plate dimensions needs more heat flux to vanish natural frequency than larger plate dimensions for the same boundary conditions.
2. As aspect ratio increases, heat flux (q) increases to reach vanishing heating load for the same boundary conditions.
3. As more restricting boundary conditions are used, the less values of heat flux will be needed to reach vanishing heating load for the same plate dimensions, i.e. the more restricting boundary conditions, the more sensitive plate to heating load.
4. The vanishing heating load of natural frequency always appear in sequentially manner.
5. An increase in aspect ratio (b/a) at constant (b) led to natural frequency increasing.

7. References

1. Danilovskay V.I., "Thermal stresses in elastic half space occurring due to heating of its surface". Prikladnaja Mathematika and Mechanika, 1950, Vol.14, No 3, 316-318.
2. James Manson “Calculating frequency response functions for uncertain systems using complex affine analysis”. Journal of Sound and Vibration,288(3, 6): 487-521,2005.
3. Xiaogeng Tian (A Direct finite element method study of generalized thermo elastic problems) International Journal of Solids and Structures, 43 2050–2063, (2006).
4. Kulik A.I., Prichodskoy V.I., (Thermal field of a plate with a heating source), USSR, Kiev, No 1, 43-46, 2007.
5. Wael Rasheed, (Linear Dynamic Thermoelasticity of Rectangular Plates) Mechanical Engineering. Baghdad, PHD thesis, 2008.
6. Naser S. Al-Huniti, M. A. Al-Nimr and M. M. Meqdad (Thermally induced vibration in thin plate under the wave heat conduction model) Journal of Thermal Stresses, 26: 943–962, 2003 Taylor & Francis Inc.2011.
7. B. H. Jeon, (Free Vibration Characteristics of Rectangular Plate under Rapid Thermal Loading) Department of Mechanical Design Engineering, Chungnam National University, Korea, 2012.
8. Husam A. Kareem, (Evaluation of natural frequencies of aluminum alloy 7075-T6 under different heat sources), Department of mechanical engineering, University of Technology, PH.D Thesis, 2015.
9. M. Necati Oisizk “Heat Conduction” Department Of Mechanical and Aerospace Engineering, North Carolina State University, published by john Wiley, 1993.
10. Arthur W. Leissa, (Vibration of Plates), Ohio State University, Columbus. Scientific and Technical Information, Division Office of Technology Utilization National Aeronautics and Space Administration, Washington, D.C.1969.